PCCP

Cite this: *Phys. Chem. Chem. Phys.*, 2012, **14**, 15429–15437

www.rsc.org/pccp

PAPER

Ultrafast dynamics of the indoline dye D149 on electrodeposited ZnO and sintered ZrO_2 and TiO_2 thin films

Kawon Oum,[a] Peter W. Lohse,†[a] Oliver Flender,[a] Johannes R. Klein,[a] Mirko Scholz,[b] Thomas Lenzer,*[a] Juan Du[c] and Torsten Oekermann‡[c]

Received 23rd August 2012, Accepted 27th September 2012
DOI: 10.1039/c2cp42961f

The ultrafast photoinjection and subsequent relaxation steps of the indoline dye D149 were investigated in detail for a mesoporous electrodeposited ZnO thin film and compared with experiments on sintered TiO_2 and ZrO_2 thin films, all in contact with air, using pump–supercontinuum probe (PSCP) transient absorption spectroscopy in the range 370–770 nm. D149 efficiently injects electrons into the ZnO surface with time constants from $\leq$70 fs (time-resolution-limited) up to 250 fs, without the presence of slower components. Subsequent spectral dynamics with a time constant of 20 ps and no accompanying change in the oscillator strength are assigned to a transient Stark shift of the electronic absorption spectrum of D149 molecules in the electronic ground state due to the local electric field exerted by the $D149^{\bullet+}$ radical cations and conduction band electrons in ZnO. This interpretation is consistent with the shape of the relaxed PSCP spectrum at long times, which resembles the first derivative of the inverted steady-state absorption spectrum of D149. In addition, steady-state difference absorption spectra of $D149^{\bullet+}$ in solution from spectroelectrochemistry display a bleach band with distinctly different position, because no first-order Stark effect is present in that case. Interference features in the PSCP spectra probably arise from a change of the refractive index of ZnO caused by the injected electrons. The 20 ps component in the PSCP spectra is likely a manifestation of the transition from an initially formed bound $D149^{\bullet+}$–electron complex to isolated $D149^{\bullet+}$ and mobile electrons in the ZnO conduction band (which changes the external electric field experienced by D149) and possibly also reorientational motion of D149 molecules in response to the electric field. We identify additional spectral dynamics on a similar timescale, arising from vibrational relaxation of $D149^{\bullet+}$ by interactions with ZnO. TiO_2 exhibits similar dynamics to ZnO. In the case of ZrO_2, electron injection accesses trap states, which exhibit a substantial probability for charge recombination. No Stark shift is observed in this case. In addition, the spectroelectrochemical experiments for $D149^{\bullet+}$ in dichloromethane and acetonitrile, which cover the spectral range up to 2000 nm, provide for the first time access to its complete $D_0 \rightarrow D_1$ absorption band, with the peak located at 1250 and 1055 nm, respectively. Good agreement is obtained with results from DFT/TDDFT calculations of the $D149^{\bullet+}$ spectrum employing the MPW1K functional.

1. Introduction

Dye-sensitized solar cells (DSSCs) have emerged as a promising class of photovoltaic units with the potential of low-cost production.[1–3] The top efficiency of such devices has currently reached 12.3%, employing a mesoporous TiO_2 electrode co-sensitized with Zn-porphyrin and cyclopentadithiophene dyes and a cobalt(II/III) based redox electrolyte.[4,5]

Another convenient material for the mesoporous electrode in a DSSC is ZnO, which has a band gap of 3.2 eV and a conduction band edge position of −4.3 eV, both similar to TiO_2.[6–8] Direct low-temperature fabrication of highly porous crystalline ZnO films from aqueous solution has been achieved by co-electrodeposition with water soluble dyes, *e.g.* eosin Y, as structure-directing additives and subsequent removal of the dye by treatment with aqueous KOH.[9–11] Subsequent readsorption of another dye with a broad absorption band and a high absorption coefficient results in the formation of a

[a] *Universität Siegen, Physikalische Chemie, Adolf-Reichwein-Str. 2, 57076 Siegen, Germany. E-mail: lenzer@chemie.uni-siegen.de; Fax: +49 271 740 2805; Tel: +49 271 740 2803*
[b] *Max-Planck-Institut für biophysikalische Chemie, Am Fassberg 11, 37077 Göttingen, Germany*
[c] *Institut für Physikalische Chemie und Elektrochemie, Leibniz-Universität Hannover, 30167 Hannover, Germany*
† Current address: Department of Physical and Analytical Chemistry – Ångström Laboratory, Uppsala University, Box 259, 751 05 Uppsala, Sweden.
‡ Current address: Friemann & Wolf Batterietechnik GmbH, Industriestr. 22, 63654 Büdingen, Germany.

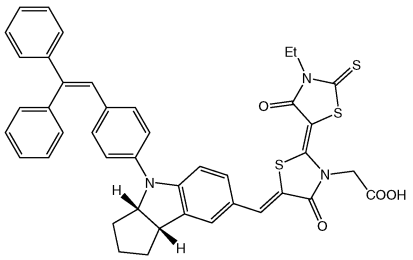

Fig. 1 Chemical structure of indoline D149.

sensitized ZnO electrode, which currently reaches efficiencies of up to 5.6% in DSSCs, with the added advantage that the low-temperature process opens up applications for flexible plastic-based devices.[12] For sensitization, metal-free dyes have come into the focus as an alternative for the frequently used ruthenium complexes. For instance, indoline derivatives with extended conjugated systems, such as the dye D149 used here (see Fig. 1), have received considerable attention, because of their high extinction coefficient and their broad absorption reaching into the red range of the spectrum.[13–15]

The timescale of photoinduced electron injection into the mesoporous semiconductor oxide surface is a key parameter for the efficiency of a DSSC. Injection processes have been studied for a variety of sensitized systems.[16–18] For sintered ZnO surfaces several studies exist,[19–26] however, electron injection has not yet been investigated for electrodeposited ZnO. In addition, information on the ultrafast dynamics of indoline dyes on ZnO surfaces is lacking, and there has been so far only one study of the femto- to picosecond dynamics of D149 on TiO_2.[27]

Here we characterize the ultrafast photoinjection and subsequent relaxation steps of the indoline dye D149 on an electrodeposited ZnO surface using ultrafast broadband transient absorption spectroscopy from the UV to the near IR and compare it with the dynamics on ZrO_2 and TiO_2. We find evidence for the transient build-up of a local Stark effect,[28–30] where the electric field exerted by the $D149^{\bullet+}$ radical cations and injected electrons influences the ground-state absorption spectrum of D149. In addition, undulatory structure in the transient spectra can be traced back to injected electrons modifying the optical response of the thin film. We also characterize the differential absorption spectrum of $D149^{\bullet+}$ by spectroelectrochemistry up to 2000 nm.

2. Experimental

2.1 Preparation of ZnO, TiO_2 and ZrO_2 thin films

Details of the preparation procedure for the ZnO films can be found in previous publications.[9,31,32] Briefly, glass substrates coated with fluorine-doped tin oxide (FTO, 10 Ω square^{-1}, Asahi Glass) were first cleaned with acetone, ethanol and distilled water and then etched in 2 M nitric acid for 2 min. ZnO/eosin Y (= EY) hybrid films were then electrodeposited from an oxygen-saturated aqueous solution (T = 70 °C), which contained 0.1 M KCl, 5 mM $ZnCl_2$ and 80 μM eosin Y, onto the FTO substrate employing a rotating disk setup (300 rpm) featuring an active area of *ca.* 2 cm^2. A Zn wire and an Ag/AgCl electrode were employed as counter and reference electrode, respectively. Deposition for 30 min at −0.91 V *vs.* Ag/AgCl (= −1.00 V *vs.* SCE) resulted in a film thickness of *ca.* 2.5 μm, with the ZnO *c*-axis preferentially oriented perpendicular to the substrate surface. The films were briefly rinsed with distilled water and dried in a stream of air. EY was desorbed by placing the as-deposited ZnO/EY films in an aqueous KOH solution (pH 10.5) for 24 h. For dye sensitization, substrates were dried at 120 °C for 1 h and immediately immersed in a 0.5 mM solution of the indoline dye D149 (Inabata UK Ltd.)[33] in acetonitrile/*tert*-butanol (1 : 1 by volume) for 30 min. This solution also contained 1 mM cholic acid as a co-adsorbant to avoid dye aggregation. The resulting sensitized ZnO film had an OD of 1.2 at the peak of the D149 absorption spectrum.

For preparation of the TiO_2 thin films, 1.2 g of TiO_2 paste (Dyesol DSL 90T) was stirred in 600 mg isopropanol and then sonicated for 20 minutes. Afterwards, doctor blading on 1 mm thick microscope slides was performed. Subsequent sintering at 450 °C resulted in highly transparent films with a thickness of *ca.* 2 μm, as determined from the interference structure of the thin film. Films were then immersed in a 0.2 mM solution of D149 in acetonitrile for 10 minutes, rinsed with fresh acetonitrile to remove unbound D149, and dried afterwards in an oven at 60 °C for 30 minutes, which had no impact on the shape of the absorption spectra. ZrO_2 films were prepared in the same manner. The required ZrO_2 paste was obtained from A. Hagfeldt as a generous gift and used as received. The typical $S_0 \rightarrow S_1$ peak absorption of the D149-sensitized sintered films was in the range of OD 0.6–1.0.

2.2 Pump–SuperContinuum Probe (PSCP) spectroscopy

Ultrafast transient absorption experiments on the dry ZnO, ZrO_2 and TiO_2 films were carried out under ambient conditions employing the PSCP setup described previously.[34–36] An overview of the principle of PSCP spectroscopy can be found elsewhere.[37] The sample was excited using a NOPA with a center wavelength of 510 or 630 nm and probed by a supercontinuum (370–770 nm) generated in a 1 mm thick CaF_2 plate. Pump and probe pulses (beam diameter 100 and 50 μm, respectively; pump beam energy *ca.* 1.5 μJ pulse^{-1}) were focused onto the sample, which was mounted on an x/y translation stage and permanently moved in a plane perpendicularly to the probe beam propagation direction so that a fresh spot on the sample was used for each laser shot. The pump–probe intensity cross-correlation time was *ca.* 70 fs as determined by using the ultrafast response of a ZnO thin film without adsorbed D149. The accuracy of the time zero determination was *ca.* 10 fs. Because of scattering of the thin films, the signal-to-noise ratio in a range of *ca.* ±15 nm around the respective pump wavelengths is reduced (*e.g.* around 510 nm in Fig. 3). No degradation of the ZnO samples was observed during the experiments: kinetic traces over the whole spectral range were identical in amplitude and shape and the absorption spectrum of the film remained unchanged even after a sequence of measurements over a period of weeks. Kinetic traces for the ZrO_2 films showed a minor reduction in amplitude (*ca.* 1% per scan), however the observed kinetics was reproducible. Photodegradation on the TiO_2 films was

more severe (*ca.* 5% per scan), yet kinetics were still reproducible and corrected by rescaling. We tentatively ascribe the reduced stability on TiO_2 and ZrO_2 to secondary reactions of the long-lived $D149^{\bullet+}$ radical cations. The differences in stability of the sensitized films will be the subject of a separate future study.

2.3 Spectroelectrochemical measurements

Spectroelectrochemistry of D149 in solution was performed using a Metrohm Autolab PGSTAT 101 potentiostat and an optically transparent thin-layer electrochemical (OTTLE) cell with 200 μm path length, featuring a Pt-disk working electrode, a Pt-gauze auxiliary electrode and an Ag-wire as a pseudoreference electrode.[38] The N_2-saturated solutions had an OD of 0.15 in acetonitrile and 0.90 in dichloromethane at the $S_0 \rightarrow S_1$ band maximum. Tetrabutylammonium perchlorate (100 mM) was used as a supporting electrolyte. UV-Vis-NIR absorption spectra were recorded on a Varian Cary 5000 spectrometer over the range 200–2000 nm. No additional features were discovered in the spectral range up to 3300 nm.

2.4 DFT/TDDFT calculations

We performed complementary DFT/TDDFT calculations to analyze the $D149^{\bullet+}$ radical cation difference absorption spectra from spectroelectrochemistry and PSCP experiments. The equilibrium structure of the $D149^{\bullet+}$ doublet ground state D_0 was optimized by density functional theory (DFT) using the B3LYP functional[39] and a 6-31G(d) basis set. Subsequently, time-dependent density functional theory (TDDFT)[40,41] was applied to this geometry for calculating the first 20 excited doublet electronic states at vertical excitation using MPW1K,[42] B3LYP and PBE0[43] functionals in combination with a 6-31+G(d) basis set. Calculations were carried out using the Gaussian 09 package.[44]

3. Results and discussion

3.1 Steady-state absorption spectra

Fig. 2 depicts normalized steady-state absorption spectra of D149. The peak position of the $S_0 \rightarrow S_1$ band in organic solvents shows only a weak variation (530 nm in acetonitrile and 543 nm in dichloromethane, both solvents containing tetrabutylammonium perchlorate at a concentration of 0.1 M for the spectroelectrochemical measurements reported in Section 3.4), in agreement with our previous study.[34] For all thin films, the spectra have a blue-shifted maximum (518 nm in the case of ZnO and ZrO_2, 524 nm for TiO_2) and exhibit a significant broadening which is probably due to heterogeneous binding environments and a certain fraction of D149 aggregates. In all cases, the background absorption of the unsensitized thin films was subtracted, which features a slow rise towards the UV (due to scattering). In addition, a pronounced increase starts at around 390 nm in the case of ZnO and TiO_2 (band gap 3.2 eV). An undulatory structure is superimposed on the absorption spectra, which is much less pronounced for ZrO_2. It can be assigned to interference features of the thin films.

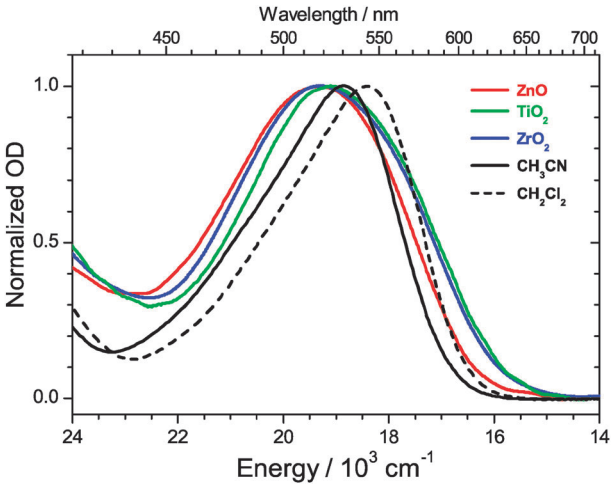

Fig. 2 Normalized steady-state absorption spectra of D149, adsorbed on an electrodeposited ZnO thin film (red line) and on sintered TiO_2 (green line) and ZrO_2 thin films (blue line), dissolved in acetonitrile (black solid line) and in dichloromethane (black dashed line). In the latter two cases, the solutions contained additional tetrabutylammonium perchlorate as a supporting electrolyte for spectroelectrochemistry (100 mM).

3.2 Transient absorption spectra of D149 on ZnO

Fig. 3 contains PSCP spectra of D149 adsorbed on ZnO upon excitation to the S_1 state at 510 nm (very similar results are obtained for the TiO_2 films). At early times (upper panel, −0.30 to 0.05 ps), negative $S_0 \rightarrow S_n$ ground state bleaching (GSB) occurs which resembles the inverted steady-state absorption spectrum of D149 (Fig. 2). In addition, $S_1 \rightarrow S_0$ stimulated emission (SE) is observed at around 540 nm. At the same time, transient excited state absorption (ESA) appears at around 430 nm and above 600 nm. The shape resembles transient spectra of the S_1 state of D149 in organic solvents at early times measured in our previous PSCP study.[34] Yet, the appearance of characteristic spectral features in the range 600–750 nm already signals the very fast formation of an additional species, which has an absorption resembling the doublet ground state D_0 of the $D149^{\bullet+}$ radical cation produced after electron injection.[28,45] Therefore, it is reasonable to assume that a substantial part of electron injection already occurs within the 70 fs time resolution of the current experiments. In fact, as will be shown below, the superimposed regular structure arises from such photoinjected electrons modifying the refractive index of the mesoporous ZnO.[46]

In the middle panel (0.1–1.0 ps) of Fig. 3, the SE quickly decays, and this is accompanied by a decay of the ESA band above 600 nm. The essentially unchanged GSB below 410 nm suggests that this decay cannot be due to recombination of a fraction of cations with some of the already injected electrons reforming D149 in the ground electronic state S_0. Instead, the global analysis of the PSCP spectra presented below is consistent with the interpretation that additional slower electron injection processes are present which result in a decrease of the GSB amplitude at around 540 nm due to superimposed absorption of the $D149^{\bullet+}$ radical cation in this

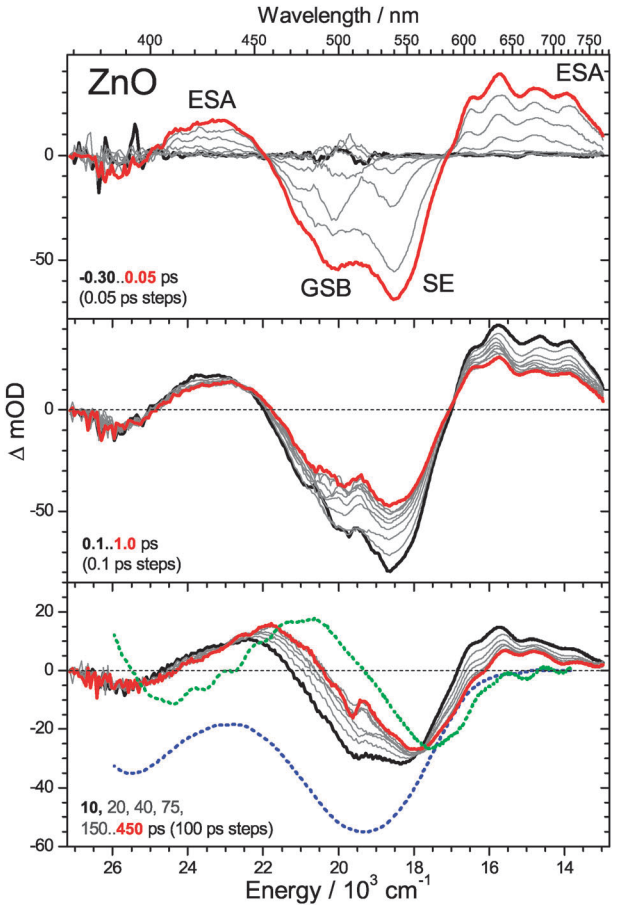

Fig. 3 Transient PSCP absorption spectra of indoline D149 on an electrodeposited ZnO thin film. Laser excitation at 510 nm. The dashed blue line in the bottom panel represents the scaled and inverted steady-state absorption spectrum of D149 on ZnO from Fig. 2. The dashed green line is the scaled first derivative of the inverted steady-state absorption spectrum.

spectral range. Thus, the ESA decay above 600 nm must be due to weaker ESA of $D149^{\bullet+}$ compared to the ESA of the S_1 state of D149. The global analysis (Section 3.3) provides a time constant of 250 fs for this slower part of electron injection.

On longer timescales (bottom panel) of Fig. 3, we observe interesting additional dynamics: an increase of absorption in the range 450–540 nm and a decrease of absorption above 570 nm. Notably, the band integral covering the range 370–770 nm stays constant, and also the energetic positions of the peaks above 580 nm remain almost unchanged. As will be discussed in the following section, these dynamics are most likely due to a transient Stark shift of the $S_0 \rightarrow S_n$ spectrum of D149 with additional spectral contributions from collisional cooling of vibrationally excited $D149^{\bullet+}$ at larger wavelengths.

In Fig. 4, we compare representative kinetic traces of D149 on ZnO with our previous experiments for D149 in the solvent methanol to highlight the completely different dynamics.[34] At 581 nm (A), the methanol transient first exhibits formation of $S_1 \rightarrow S_n$ ESA. The characteristic curvature around the peak is due to solvation dynamics arising from the transient red-shift of the superimposed weaker $S_1 \rightarrow S_0$ SE. The signal then decays to zero due to internal conversion (IC, $S_1 \rightarrow S_0$) with a

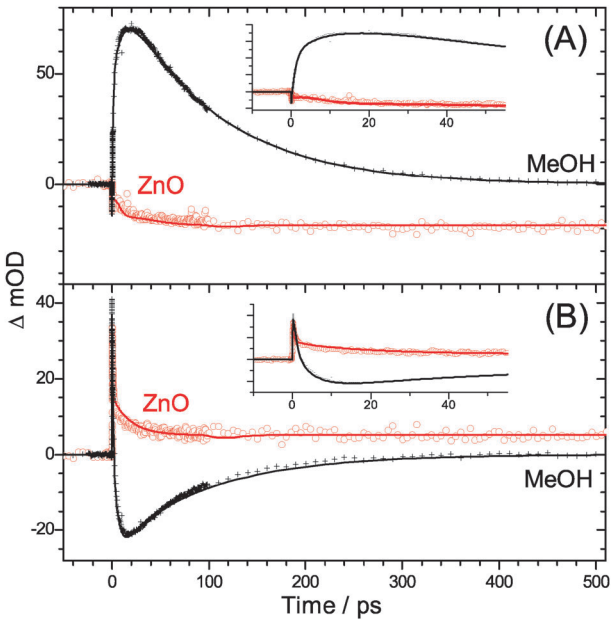

Fig. 4 Selected kinetic traces for the dynamics of D149 on ZnO (red) and in methanol (black) at (A) $\lambda_{probe} = 581$ nm, (B) $\lambda_{probe} = 693$ nm. $\lambda_{pump} = 510$ nm. The insets show magnifications at early times. Solid lines are results from the global kinetic analysis.

time constant of 99 ps. In contrast, for ZnO (581 nm) we see an instantaneous drop due to formation of GSB. The origin of the curvature (Stark shift and radical cation cooling) will be discussed in Section 3.3. The GSB then stays at a constant level showing that the original D149 population was depleted by electron injection and does not recover on this timescale.

At 693 nm (B), $S_1 \rightarrow S_n$ ESA in methanol is formed initially which is then transformed into $S_1 \rightarrow S_0$ SE because of the transient Stokes shift of the SE band. Finally, the signal decays due to IC from S_1 to S_0. In contrast, ZnO stimulated emission of D149 is never observed in this spectral region because the S_1 state is so short-lived and dipolar solvation dynamics is of course absent on ZnO. Consequently, we first see $S_1 \rightarrow S_n$ ESA of D149 which is quickly decaying due to electron injection. Afterwards, the same type of curvature is found as in (A), and the absorption then stays at a constant level (arising from $D149^{\bullet+}$).

3.3 Global analysis of transient spectra of D149 on ZnO

The transient absorption spectra in Fig. 3 were analyzed globally using the scheme

$$S_0(D149) \xrightarrow{h\nu_{pump}} S_1(D149) \quad (1)$$

$$S_1(D149) \xrightarrow{k_{inj}} D_0(D149^{\bullet+}) + e^-(ZnO) \quad (2)$$

$$D_0(D149^{\bullet+}) + e^-(ZnO) \xrightarrow{k_{rec}} S_0(D149) \quad (3)$$

The experiments were carried out on a sensitized ZnO film in air, which is not in contact with a redox electrolyte. In this case, the recombination rate constant k_{rec} of $D149^{\bullet+}$ with electrons in ZnO in step (3) is apparently slow ($\gg 1$ ns), because no decay of the PSCP transients is seen up to 1 ns.

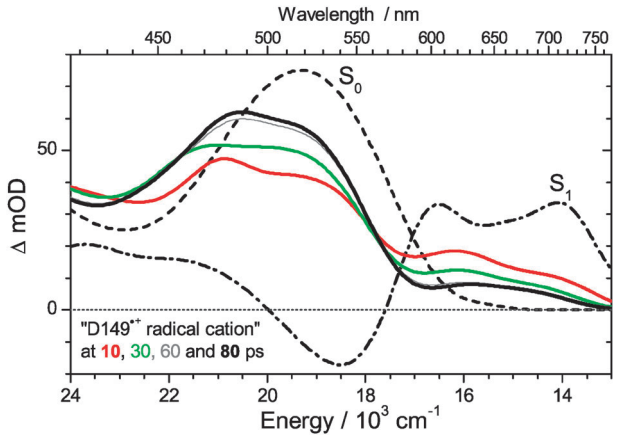

Fig. 5 Species-associated spectra from global analysis of the ultrafast transient absorption data for D149 on ZnO. The time-dependent spectrum termed "D149$^{\bullet+}$ radical cation" features a Stark shift of the $S_0 \rightarrow S_n$ band of D149 and vibrational relaxation of D149$^{\bullet+}$.

Possible spectral contributions of the photoinjected electrons will be discussed below.[23,46,47]

In the current study, all species-associated spectra were represented by a sum of Gaussian functions. A time-independent spectrum was sufficient to describe the S_1 state of D149 due to its very short lifetime on the ZnO thin film. Because of this ultrashort lifetime and the fact that no solvent molecules are in contact with the dye, it is also reasonable to assume that the S_1 spectrum of D149 on the ZnO thin film closely resembles early-time S_1 spectra previously measured in our PSCP experiments of D149 in organic solvents.[34] These are characterized by weak stimulated emission appearing at around 540 nm (slightly to the red of the peak for the ground state bleach) and by broad unstructured excited-state absorption below 500 nm and above 560 nm (Fig. 5).

To understand the slower dynamics in the bottom panel of Fig. 3, it is necessary to consider two main processes which will likely influence the transient spectra: Cappel *et al.* reported that local electric fields originating from the D149$^{\bullet+}$ radical cations and photoinjected electrons induce a Stark effect which shifts the $S_0 \rightarrow S_1$ absorption band of D149 to shorter wavelengths. This was confirmed in photoinduced absorption (PIA) experiments for D149 on mesoporous TiO_2 films, which exhibited a characteristic bleach feature centered at *ca.* 600 nm.[28] A similar spectral feature was observed before in the study of Snaith *et al.*[48] The effect is also supported by DFT/TDDFT calculations, in which a characteristic blue-shift of the D149 absorption spectrum in the presence of an external electric field was found.[28]

The second process to be considered is collisional cooling of vibrationally excited D149$^{\bullet+}$ radical cations which are produced after electron injection. Because injection will occur from the neutral D149 geometry, the resulting D149$^{\bullet+}$ in the D_0 state will certainly be produced in a non-equilibrium configuration, *i.e.*, vibrationally excited. Afterwards, this vibrational excess energy needs to be dissipated by interactions with the ZnO surface.

In our global analysis we used a simplified approach to describe these processes by employing a time-dependent D149$^{\bullet+}$ radical cation spectrum. Transient changes in this spectrum will therefore reflect changes of the radical cation spectrum due to vibrational relaxation and superimposed changes in the $S_0 \rightarrow S_n$ spectrum of D149 molecules induced by the electric field exerted by these radical cations and the injected electrons.

In the fitting procedure, the time constant for the injection step (2) $\tau_{inj} = k_{inj}^{-1}$ and for the subsequent changes of the D149$^{\bullet+}$ spectrum ($\tau_{relax} = k_{relax}^{-1}$) were optimized to obtain the best fit with a minimum set of parameters. The spectra obtained from the global analysis are presented in Fig. 5. The initially broad D149$^{\bullet+}$ spectrum shows a decrease above 560 nm and an increase between 430 and 560 nm, with an isosbestic point at 560 nm. Spectral development occurs with a time constant $\tau_{relax} \approx 20$ ps. This means that one observes an increase in absorption slightly to the blue of the $S_0 \rightarrow S_1$ absorption maximum of D149, and a loss of amplitude on the red edge of the $S_0 \rightarrow S_1$ band of D149. The resulting spectrum looks also different from the D149$^{\bullet+}$ spectra obtained from spectroelectrochemistry, which will be discussed in Section 3.4. This leads us to the conclusion that these spectral dynamics are likely dominated by the "local Stark effect" proposed by Cappel *et al.*[28] and Meyer and co-workers.[29,30] Further support comes from the study of Cappel *et al.*[28] They showed that PIA spectra of D149 on TiO_2 were dominated by the first-order Stark effect: for the limiting case of aligned D149 molecules and an electric field acting normal to the surface, the change in absorbance (ΔOD) should be proportional to the first derivative of the steady-state absorption spectrum of D149.[28] The scaled derivative of the inverted steady-state absorption spectrum is depicted in Fig. 3 (bottom panel) as a dashed green line. Its shape is remarkably similar to the "relaxed" PSCP spectrum at 450 ps, yet it is clearly further red-shifted. This indicates that complete uniform alignment of all D149 molecules on the ZnO surface is not achieved, and this is reasonable, because electrodeposited mesoporous ZnO does not represent a flat surface.[12]

It is interesting that the blue-shift of the $S_0 \rightarrow S_1$ band does not appear instantaneously upon photoinjection, but gradually builds up with a time constant of 20 ps. Earlier studies for two dyes on ZnO suggest that after photoinjection first a bound electron–cation complex is quickly formed which possesses a "cation-like" spectrum. Afterwards, this complex dissociates into the cation and a mobile electron in the ZnO conduction band.[21,22,25,26] This mechanism is supported by the delayed appearance of mobile electrons (on the several 10 ps timescale) in transient THz experiments.[26] We speculate that such a process could be one reason for the gradual establishment of the local Stark field. In addition, the dipolar D149 molecules will need some time to align to this external electric field, which will require reorientational motion.

Particularly interesting is also the fact that the PSCP spectra in the bottom panel of Fig. 3 show the same undulatory structure as the first derivative of the steady-state absorption spectrum (see *e.g.* the region above 580 nm) and that these peaks in the PSCP spectra are already present at early times (Fig. 3, top) and essentially do not shift with time. The structure of the derivative arises from the weak interference pattern in the steady-state absorption spectrum of the *ca.* 2.5 μm thick ZnO film.

Normally, this structure should cancel out in differential absorption spectra. The fact that it is however still seen in the PSCP spectra suggests that there must be a subtle change in the refractive index of ZnO after photoexcitation of the dye. To explain this, we refer to an earlier study of Bauer *et al.*[46] In that case, a similar interference pattern was observed in differential absorption spectra from spectroelectrochemistry of a mesoporous ZnO electrode (without attached dye) upon application of a negative potential. The result was interpreted in terms of a flow of electrons into the electrode, which change the optical properties (*i.e.* refractive index) of the thin film. As we see a very similar structure already in the early PSCP spectra (Fig. 3, top), we take this as additional evidence that the photoinduced injection of electrons into ZnO is extremely fast. Beside the undulatory structure and weak absorption above 620 nm, Bauer *et al.* also observed a pronounced Moss–Burstein bleach feature of the ZnO thin film below *ca.* 400 nm.[46] Although this is already close to the lowest probe wavelengths covered in our current PSCP experiments, it appears as if there is not such a strong bleach feature for our D149/ZnO sample.

We note that to some extent the transient spectra in Fig. 5 also indicate relaxation of vibrationally "hot" $D149^{\bullet+}$ on the ZnO surface: particularly, the absorption decay in the range above 650 nm, where there is no appreciable influence of the $S_0 \rightarrow S_1$ spectrum of D149, can be hardly explained by a local Stark effect. Also, the observed spectral narrowing, the conservation of the oscillator strength of the band and the 20 ps timescale of the process would be consistent with vibrational cooling, in agreement with solution studies.[35,49–52] In the present case, vibrational relaxation will occur by interaction of the attached $D149^{\bullet+}$ with the ZnO surface (vibration-to-phonon energy transfer, both "intermolecular" as well as by coupling through the carboxyl anchor group) and with adjacent D149 molecules. We did not attempt to further deconvolve the transient spectra in Fig. 5 into a "pure $D149^{\bullet+}$ spectrum" and a "Stark-shifted $S_0 \rightarrow S_n$ spectrum".

We also note that similar PSCP spectra and simulations are obtained for excitation on the red edge of the $S_0 \rightarrow S_1$ band (630 nm), the only difference being that the broadening of the transient "$D149^{\bullet+}$ spectrum" was less pronounced than in Fig. 5: this is understandable, because excitation at 630 nm with the same pulse energy excites less D149 molecules (smaller absorption coefficient, see Fig. 2), resulting in a smaller amount of cations/electrons and thus a less pronounced Stark effect. Also, the initial vibrational excitation of the generated radical cations is *ca.* 3700 cm^{-1} smaller for excitation at 630 nm, resulting in narrower "hot" $D149^{\bullet+}$ spectra.

3.4 $D149^{\bullet+}$ radical cation spectrum

We also performed spectroelectrochemical experiments in dichloromethane and acetonitrile solutions to determine steady-state difference absorption spectra of $D149^{\bullet+}$ for comparison with our transient PSCP data. These are depicted in Fig. 6 as red and blue lines, respectively. Studies of $D149^{\bullet+}$ on TiO_2 over the spectral range 400–1100 nm were reported previously.[28,45] Our current experiments extend the spectral range considerably, providing for the first time access to the complete $D_0 \rightarrow D_1$ absorption band of $D149^{\bullet+}$ located in the near IR. Its peak is located at 1250 nm in dichloromethane and at 1055 nm in acetonitrile which suggests a quite substantial influence of solvent polarity on the $D_0 \rightarrow D_1$ transition energy.

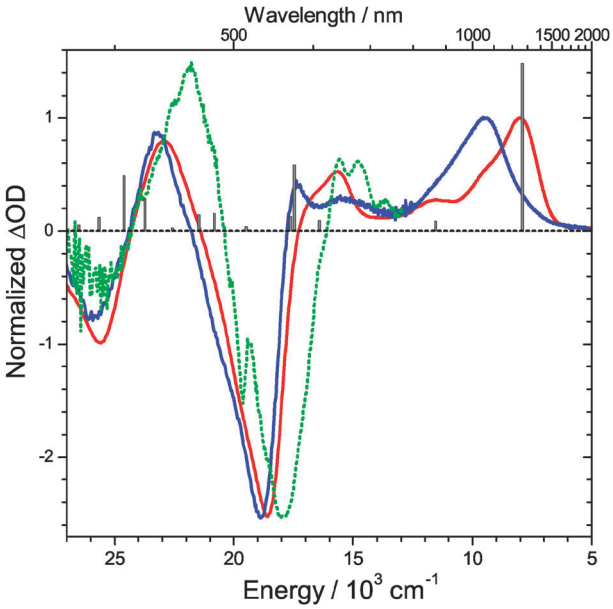

Fig. 6 Differential absorption spectra of the $D149^{\bullet+}$ radical cation from spectroelectrochemistry in dichloromethane (red line) and acetonitrile (blue line) compared with the "relaxed" PSCP spectrum on ZnO at 450 ps (dotted green line). Grey columns mark the positions of the $D_0 \rightarrow D_n$ electronic transitions obtained from DFT/TDDFT calculations employing the MPW1K functional (Table 1), where the relative amplitudes are proportional to the respective oscillator strengths.

We carried out DFT/TDDFT calculations to assign the electronic transitions in the $D149^{\bullet+}$ spectrum. Best agreement with the experimental data was achieved for the MPW1K functional, whereas calculations employing B3LYP and PBE0 functionals appear to underestimate the transition energies systematically (see Table 1 for a summary of the 20 lowest electronic transitions). Stick spectra for the MPW1K results are overlaid in Fig. 6. The $D_0 \rightarrow D_1$ transition wavelength is very well reproduced. The small broad peak at around 870 nm in the dichloromethane spectrum can be assigned to the $D_0 \rightarrow D_2$ transition, with a tail extending down to 650 nm. Further to the blue, a group of three peaks dominated by $D_0 \rightarrow D_5$ emerges, which is located in the bleach region of the PSCP spectrum (dotted green line). Another group of peaks ($D_0 \rightarrow D_{10,12,15,16}$) is responsible for the prominent absorption feature in the 410–470 nm region on top of the D149 bleach.

Particularly interesting is the comparison between the spectroelectrochemistry results and the "relaxed" PSCP spectrum at 450 ps. The bleach region of the PSCP spectrum is red-shifted by about 600 cm^{-1} with respect to the dichloromethane spectrum (and also the spectra of $D149^{\bullet+}$ on TiO_2 published previously[28,45]). In addition, the PSCP ESA band centered at *ca.* 460 nm has an increased amplitude. As mentioned above, we take both observations as a strong indication of the presence of a local Stark effect in the PSCP spectra, which shifts the $S_0 \rightarrow S_1$ transition of D149 to shorter wavelengths.

Table 1 Results of DFT/TDDFT calculations for the $D149^{\bullet+}$ radical cation: wavelengths of the first 20 vertical electronic transitions using B3LYP, PBE0 and MPW1K functionals, and oscillator strengths *f* for calculations using the MPW1K functional

$D_0 \rightarrow D_n$	λ/nm (B3LYP)	λ/nm (PBE0)	λ/nm (MPW1K)	*f* (MPW1K)
1	1555	1509	1263	0.9342
2	1292	1093	866	0.0560
3	1037	1005	662	0.0001
4	723	670	609	0.0603
5	697	659	572	0.3681
6	681	640	567	0.0820
7	654	633	517	0.0065
8	639	617	513	0.0251
9	630	590	495	0.0001
10	559	555	480	0.1001
11	551	530	474	0.0033
12	519	508	466	0.0918
13	514	497	443	0.0183
14	512	481	425	0.0000
15	495	476	421	0.1841
16	494	473	406	0.3100
17	465	447	403	0.0002
18	457	437	390	0.0770
19	455	429	383	0.0008
20	444	422	377	0.0367

3.5 Transient absorption of D149 on ZrO_2 and TiO_2

We also carried out experiments for D149 adsorbed on ZrO_2, which represents a semiconductor oxide surface with a much larger band gap (*ca.* 5 eV) than ZnO (*ca.* 3.2 eV). Fig. 7 contains PSCP results for the dynamics of D149 on ZrO_2 after photoexcitation at 510 nm, where spectra were recorded at the same time delays as in Fig. 3. The dynamics up to the first picosecond (top and middle panels) resemble those of ZnO. The fast decay of the GSB and ESA bands above 450 nm (*ca.* 250 fs time constant) in the middle panel is accompanied by essentially no change in spectral features in the 390–420 nm region. Therefore we assign these dynamics to the primary electron injection step (formation of a cation–electron complex), as in ZnO.

The quite similar early-time behavior of ZrO_2 and ZnO might be at first sight surprising. In the case of bulk ZrO_2, the conduction band edge is reportedly 1.0–1.5 eV higher than for TiO_2 (anatase), however the difference was estimated to be much smaller in the case of the nanocrystalline systems, about 0.5 eV.[53] In addition, it can be estimated that vertical $S_0 \rightarrow S_1$ excitation provides access to D149 levels which should be located at *ca.* 0.3 eV above the conduction band edge of ZnO.[54] Therefore, while electron injection appears to be less facile for ZrO_2, it could definitely be possible, especially into trap states located below the conduction band edge.[6,55–57]

The dynamics at longer times can be found in the bottom panel and is different from ZnO in two respects: here, one does not observe such distinct rise and decay features in the ESA (430 nm) and GSB (530 nm) bands (appearing like a red-shift of the whole spectrum in Fig. 3). This suggests, that separation of the initially formed close complexes of trapped electrons and cations does not easily occur, because of the unfavorable energetic location of the conduction band of ZrO_2. The build-up of a local Stark field acting on ground-state D149 (S_0) therefore appears to be largely suppressed. There are also no clear interference features of the thin film in these PSCP spectra. One reason for this is the fact that the undulations in the steady-state absorption spectrum for ZrO_2 are much weaker than in the case of ZnO, which will result in a much smaller amplitude of such features. Also, the refractive index change caused by electron–cation complexes might be considerably reduced in the case of ZrO_2 (Fig. 7).

Also, one observes a clear decay (time constant *ca.* 30 ps), most easily seen in the GSB band at around 540 nm. A reasonable explanation is the recombination of a fraction of the electron–cation complexes reforming D149 in S_0.[55] The red-shift of the ESA band above 640 nm looks similar to the spectral development on ZnO (and also TiO_2) in this wavelength region. We therefore assign this process to vibrational relaxation of the electron–cation complex, which should have a spectral signature similar to isolated $D149^{\bullet+}$.[26] Fits in this wavelength region provide a time constant of 25 ps (for a comparison of ZrO_2, ZnO and TiO_2 see Fig. 8). For ZrO_2, in this spectral region we therefore observe a decay of the electron–cation complexes due to charge recombination and also vibrational cooling, both with a similar time constant. We also note, that only for ZrO_2 there is a very slow decay of the whole spectrum with small amplitude, roughly with a time constant of 1 ns (not reliably measurable within our time window). This could be due to recombination of longer-lived

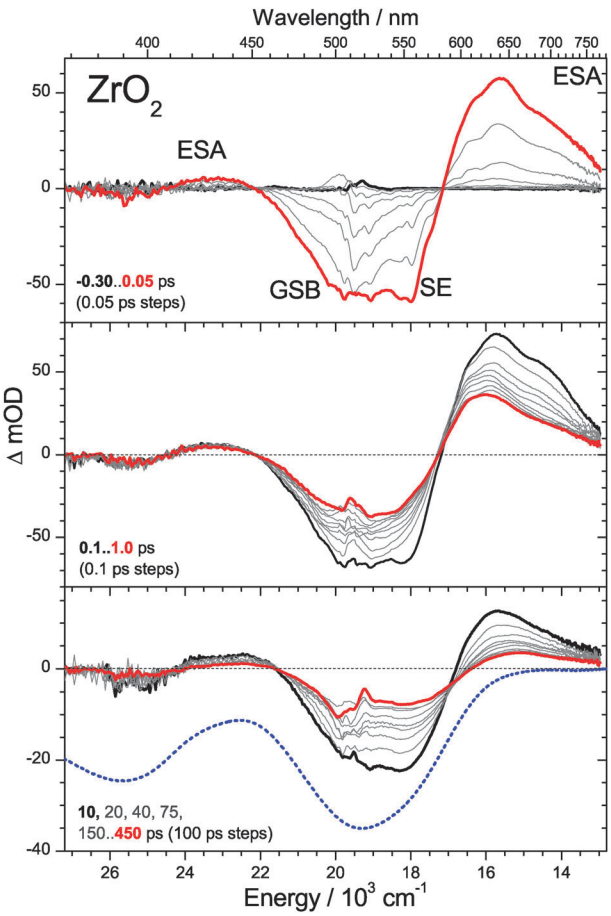

Fig. 7 Transient PSCP absorption spectra of indoline D149 on a ZrO_2 thin film. Laser excitation at 510 nm. The dashed line in the bottom panel represents the scaled and inverted steady-state absorption spectrum of D149 on ZrO_2 from Fig. 2.

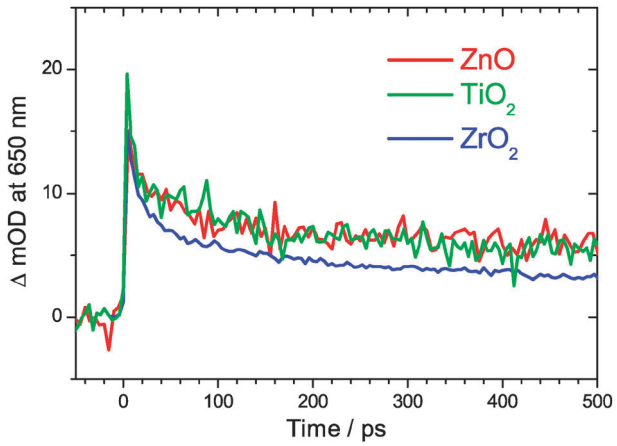

Fig. 8 Transient PSCP absorption signals of indoline D149 attached to ZnO, TiO_2 and ZrO_2 thin films. λ_{probe} = 650 nm, λ_{pump} = 510 nm.

electron–cation complexes or internal conversion of a smaller fraction of D149 molecules in S_1 which did not undergo electron injection. For the latter process, the lifetime would be in line with those previously measured by us in less polar solvents (*e.g.* 720 ps in THF).[34]

4. Conclusions

In summary, we have shown that the indoline dye D149 very efficiently injects electrons on an ultrafast timescale ($\leq$250 fs) into a highly porous electrodeposited ZnO thin film, initially forming an e^-–D149$^{\bullet+}$ complex. The same is observed for sintered ZrO_2 and TiO_2 surfaces, where only in the former case electrons are obviously trapped and have the chance to recombine to repopulate D149 in S_0 on longer timescales.

For ZnO (and TiO_2), the e^-–D149$^{\bullet+}$ complex dissociates and forms mobile electrons in the conduction band. We believe that we track this formation of mobile electrons in terms of a characteristic spectral evolution in the PSCP spectra with a time constant of *ca.* 20 ps, which signals the build-up of a local electric field (Stark effect)[28–30] acting on unexcited D149 molecules in S_0. This is also supported by the shape of the relaxed PSCP spectrum which is similar to that of the first derivative of the steady-state (bleach) absorption spectrum. The spectral dynamics possibly also contain contributions of D149 molecules on the thin film, which reorient in response to the newly forming electric field. Additional undulatory structure in the PSCP spectra is likely due to the change of the refractive index of ZnO due to injection of electrons.[46]

A spectral component with a similar time constant observed in the red region of the spectrum (where a Stark shift cannot be present) is likely due to vibrational cooling of D149$^{\bullet+}$ by interactions with the surface (collisional or through-bond energy transfer to ZnO). We believe that it is of general importance to consider the possible presence of such processes on the several picosecond timescale in the interpretation of any ultrafast transient absorption experiment dealing with electron injection from dye molecules into thin films.

The very efficient injection of electrons into highly porous electrodeposited ZnO suggests a negligible disturbance of the injection process by D149 aggregates.[19,20,58] Obviously, aggregation of the dye molecules on the ZnO surface was successfully suppressed by the addition of cholic acid as a co-adsorbent in the dye solution. We plan to study the influence of the co-adsorbant on the dynamics of the three thin film systems in a more systematic way in a forthcoming publication.

A substantial loss of injected electrons by recombination in the picosecond range was reported previously, *e.g.*, 75% in the study of Sundström and co-workers for a Zn-porphyrin dye on ZnO nanoparticles.[26] In that case, the initially formed e^-–dye complex obviously had a high chance of recombination. Such a behavior is not seen in the current study. This is most likely due to favorable electronic properties of the indoline dye, with the LUMO located close to the anchoring group (resulting in facile electron injection) and the HOMO also more delocalized toward the "opposite end" of the dye, decreasing the possibility for charge recombination by "hole trapping".[3,54,59]

In future investigations, it will also be interesting to probe the population of mobile charge carriers in D149-sensitized electrodeposited ZnO films using time-resolved THz spectroscopy: this way, one could test if one observes the appearance of mobile electrons on the 20 ps timescale.[25,26] It will also be worthwhile to extend the PSCP investigations toward ZnO thin films in contact with an electrolyte solution to investigate its influence on the ultrafast electron injection dynamics and transient Stark shift contributions to the PSCP spectra.

Acknowledgements

We would like to thank N. P. Ernsting and J. L. Pérez Lustres for extensive help during the implementation of the PSCP setup, R. Oswald for assistance during the DFT/TDDFT calculations, A. Hagfeldt for generously providing the ZrO_2 paste used for producing the respective thin films for this study, and M. Adlung and C. Wickleder for providing the programmable oven for the ZrO_2 and TiO_2 film sintering. We also thank S. I. Druzhinin for an additional spectrum of D149$^{\bullet+}$ in acetonitrile, which was used for comparison. In addition, excellent technical support from D. Gaumann, B. Meyer and M. Rabe is gratefully acknowledged. Finally, we thank the referees for their very helpful comments.

Notes and references

1 A. Hagfeldt, G. Boschloo, L. Sun, L. Kloo and H. Pettersson, *Chem. Rev.*, 2010, **110**, 6595.
2 A. Listorti, B. O'Regan and J. R. Durrant, *Chem. Mater.*, 2011, **23**, 3381.
3 M. Grätzel, *Inorg. Chem.*, 2005, **44**, 6841.
4 A. Yella, H.-W. Lee, H. N. Tsao, C. Yi, A. K. Chandiran, M. K. Nazeeruddin, E. W.-G. Diau, C.-Y. Yeh, S. M. Zakeeruddin and M. Grätzel, *Science*, 2011, **334**, 629.
5 H. N. Tsao, C. Yi, T. Moehl, J.-H. Yum, S. M. Zakeeruddin, M. K. Nazeeruddin and M. Grätzel, *ChemSusChem*, 2011, **4**, 591.
6 A. Hagfeldt and M. Grätzel, *Chem. Rev.*, 1995, **95**, 49.
7 Q. Zhang, C. S. Dandeneau, X. Zhou and G. Cao, *Adv. Mater.*, 2009, **21**, 4087.
8 J. A. Anta, E. Guillén and R. Tena-Zaera, *J. Phys. Chem. C*, 2012, **116**, 11413.
9 T. Yoshida, M. Iwaya, H. Ando, T. Oekermann, K. Nonomura, D. Schlettwein, D. Wöhrle and H. Minoura, *Chem. Commun.*, 2004, 400.
10 T. Yoshida, K. Terada, D. Schlettwein, T. Oekermann, T. Sugiura and H. Minoura, *Adv. Mater.*, 2000, **12**, 1214.

11 T. Yoshida, T. Pauporté, D. Lincot, T. Oekermann and H. Minoura, *J. Electrochem. Soc*., 2003, **150**, C608.
12 T. Yoshida, J. Zhang, D. Komatsu, S. Sawatani, H. Minoura, T. Pauporté, D. Lincot, T. Oekermann, D. Schlettwein, H. Tada, D. Wöhrle, K. Funabiki, M. Matsui, H. Miura and H. Yanagi, *Adv. Funct. Mater*., 2009, **19**, 17.
13 T. Horiuchi, H. Miura and S. Uchida, *Chem. Commun*., 2003, 3036.
14 T. Horiuchi, H. Miura, K. Sumioka and S. Uchida, *J. Am. Chem. Soc*., 2004, **126**, 12218.
15 S. Ito, S. M. Zakeeruddin, R. Humphry-Baker, P. Liska, R. Charvet, P. Comte, M. K. Nazeeruddin, P. Péchy, M. Takata, H. Miura, S. Uchida and M. Grätzel, *Adv. Mater*., 2006, **18**, 1202.
16 R. Katoh, A. Furube, A. V. Barzykin, H. Arakawa and M. Tachiya, *Coord. Chem. Rev*., 2004, **248**, 1195.
17 N. A. Anderson and T. Lian, *Annu. Rev. Phys. Chem*., 2005, **56**, 491.
18 O. Bräm, A. Cannizzo and M. Chergui, *Phys. Chem. Chem. Phys*., 2012, **14**, 7934.
19 J. B. Asbury, Y. Wang and T. Lian, *J. Phys. Chem. B*, 1999, **103**, 6643.
20 C. Bauer, G. Boschloo, E. Mukhtar and A. Hagfeldt, *J. Phys. Chem. B*, 2001, **105**, 5585.
21 A. Furube, R. Katoh, K. Hara, S. Murata, H. Arakawa and M. Tachiya, *J. Phys. Chem. B*, 2003, **107**, 4162.
22 A. Furube, R. Katoh, T. Yoshihara, K. Hara, S. Murata, H. Arakawa and M. Tachiya, *J. Phys. Chem. B*, 2004, **108**, 12583.
23 T. Yoshihara, R. Katoh, A. Furube, M. Murai, Y. Tamaki, K. Hara, S. Murata, H. Arakawa and M. Tachiya, *J. Phys. Chem. B*, 2004, **108**, 2643.
24 J. M. Szarko, A. Neubauer, A. Bartelt, L. Socaciu-Siebert, F. Birkner, K. Schwarzburg, T. Hannappel and R. Eichberger, *J. Phys. Chem. C*, 2008, **112**, 10542.
25 D. Stockwell, Y. Yang, J. Huang, C. Anfuso, Z. Huang and T. Lian, *J. Phys. Chem. C*, 2010, **114**, 6560.
26 H. Nemec, J. Rochford, O. Taratula, E. Galoppini, P. Kuzel, T. Polívka, A. Yartsev and V. Sundström, *Phys. Rev. Lett*., 2010, **104**, 197401.
27 M. Fakis, E. Stathatos, G. Tsigaridas, V. Giannetas and P. Persephonis, *J. Phys. Chem. C*, 2011, **115**, 13429.
28 U. B. Cappel, S. M. Feldt, J. Schöneboom, A. Hagfeldt and G. Boschloo, *J. Am. Chem. Soc*., 2010, **132**, 9096.
29 S. Ardo, Y. Sun, A. Staniszewski, F. N. Castellano and G. J. Meyer, *J. Am. Chem. Soc*., 2010, **132**, 6696.
30 S. Ardo, Y. Sun, F. N. Castellano and G. J. Meyer, *J. Phys. Chem. B*, 2010, **114**, 14596.
31 H. Graaf, C. Maedler, M. Kehr and T. Oekermann, *J. Phys. Chem. C*, 2009, **113**, 6910.
32 C. Boeckler, T. Oekermann, M. Saruban, K. Ichinose and T. Yoshida, *Phys. Status Solidi A*, 2008, **205**, 2388.
33 S. Ito, H. Miura, S. Uchida, M. Takata, K. Sumioka, P. Liska, P. Comte, P. Péchy and M. Grätzel, *Chem. Commun*., 2008, 5194.
34 P. W. Lohse, J. Kuhnt, S. I. Druzhinin, M. Scholz, M. Ekimova, T. Oekermann, T. Lenzer and K. Oum, *Phys. Chem. Chem. Phys*., 2011, **13**, 19632.
35 K. Golibrzuch, F. Ehlers, M. Scholz, R. Oswald, T. Lenzer, K. Oum, H. Kim and S. Koo, *Phys. Chem. Chem. Phys*., 2011, **13**, 6340.
36 T. Lenzer, S. Schubert, F. Ehlers, P. W. Lohse, M. Scholz and K. Oum, *Arch. Biochem. Biophys*., 2009, **483**, 213.
37 A. L. Dobryakov, S. A. Kovalenko, A. Weigel, J. L. Pérez Lustres, J. Lange, A. Müller and N. P. Ernsting, *Rev. Sci. Instrum*., 2010, **81**, 113106.
38 M. Krejcik, M. Danek and F. Hartl, *J. Electroanal. Chem*., 1991, **317**, 179.
39 A. D. Becke, *J. Chem. Phys*., 1993, **98**, 5648.
40 E. Runge and E. K. U. Gross, *Phys. Rev. Lett*., 1984, **52**, 997.
41 A. Dreuw and M. Head-Gordon, *Chem. Rev*., 2005, **105**, 4009.
42 M. Pastore, E. Mosconi, F. De Angelis and M. Grätzel, *J. Phys. Chem. C*, 2010, **114**, 7205.
43 C. Adamo and V. Barone, *J. Chem. Phys*., 1999, **110**, 6158.
44 M. J. Frisch, G. W. Trucks, H. B. Schlegel and G. E. Scuseria, et al., *Gaussian 09, Revision A.01*, Gaussian, Inc., Wallingford, CT (USA), 2009.
45 A. Fattori, L. M. Peter, H. Wang, H. Miura and F. Marken, *J. Phys. Chem. C*, 2010, **114**, 11822.
46 C. Bauer, G. Boschloo, E. Mukhtar and A. Hagfeldt, *Chem. Phys. Lett*., 2004, **387**, 176.
47 R. Katoh, A. Furube, K. Hara, S. Murata, H. Sugihara, H. Arakawa and M. Tachiya, *J. Phys. Chem. B*, 2002, **106**, 12957.
48 H. J. Snaith, A. Petrozza, S. Ito, H. Miura and M. Grätzel, *Adv. Funct. Mater*., 2009, **19**, 1810.
49 D. Schwarzer, J. Troe, M. Votsmeier and M. Zerezke, *J. Chem. Phys*., 1996, **105**, 3121.
50 S. A. Kovalenko, R. Schanz, H. Hennig and N. P. Ernsting, *J. Chem. Phys*., 2001, **115**, 3256.
51 D. Schwarzer, C. Hanisch, P. Kutne and J. Troe, *J. Phys. Chem. A*, 2002, **106**, 8019.
52 T. Lenzer, F. Ehlers, M. Scholz, R. Oswald and K. Oum, *Phys. Chem. Chem. Phys*., 2010, **12**, 8832.
53 B. I. Lemon, F. Liu and J. T. Hupp, *Coord. Chem. Rev*., 2004, **248**, 1225.
54 T. Le Bahers, T. Pauporté, G. Scalmani, C. Adamo and I. Ciofini, *Phys. Chem. Chem. Phys*., 2009, **11**, 11276.
55 R. Huber, S. Spörlein, J. E. Moser, M. Grätzel and J. Wachtveitl, *J. Phys. Chem. B*, 2000, **104**, 8995.
56 C. M. Olsen, M. R. Waterland and D. F. Kelley, *J. Phys. Chem. B*, 2002, **106**, 6211.
57 E. Hao, N. A. Anderson, J. B. Asbury and T. Lian, *J. Phys. Chem. B*, 2002, **106**, 10191.
58 N. A. Anderson, A. Xin and T. Lian, *J. Phys. Chem. B*, 2003, **107**, 14414.
59 J. Y. Kim, Y. H. Kim and Y. S. Kim, *Curr. Appl. Phys*., 2011, **11**, S117.